S. Zhang
State Key Laboratory of Nonlinear Mechanics (LNM),
Institute of Mechanics,
Chinese Academy of Sciences,
Beijing 100190, China;
School of Engineering Science,
University of Chinese Academy of Sciences,
Beijing 100049, China
e-mail: zhangsiyuan@imech.ac.cn

H. Song[1]
The Micromechanical Materials Modelling Group,
Institute of Mechanics and Fluid Dynamics,
TU Bergakademie Freiberg,
Freiberg 09599, Germany
e-mail: Hengxu.Song@imfd.tu-freiberg.de

S. Sandfeld
The Micromechanical Materials Modelling Group,
Institute of Mechanics and Fluid Dynamics,
TU Bergakademie Freiberg,
Freiberg 09599, Germany
e-mail: Stefan.Sandfeld@imfd.tu-freiberg.de

X. Liu[1]
State Key Laboratory of Nonlinear Mechanics (LNM),
Institute of Mechanics,
Chinese Academy of Sciences,
Beijing 100190, China;
School of Engineering Science,
University of Chinese Academy of Sciences,
Beijing 100049, China
e-mail: Xiaomingliu@lnm.imech.ac.cn

Y. G. Wei
College of Engineering,
Peking University,
Beijing 100871, China
e-mail: weiyg@pku.edu.cn

Discrete Greenwood–Williamson Modeling of Rough Surface Contact Accounting for Three-Dimensional Sinusoidal Asperities and Asperity Interaction

The Greenwood–Williamson (GW) model has been one of the commonly used contact models to study rough surface contact problems during the past decades. While this has been a successful model, it still has a number of restrictions: (i) surface asperities are spheres; (ii) the overall deformation must be assumed to be small enough, such that there is no interaction between asperities, i.e., they are independent of each other; and (iii) asperity deformation remains elastic. This renders the GW model unrealistic in many situations. In the present work, we resolve above restrictions in a discrete version of the GW model: instead of spherical asperities, we assumed that the surface consists of three-dimensional sinusoidal asperities which appear more similar to asperities on a rough surface. For single asperity mechanical response, we propose a Hertz-like analytical solution for purely elastic deformation and a semi-analytical solution based on finite element method (FEM) for elastic–plastic deformation. The asperity interaction is accounted for by discretely utilizing a modified Boussinesq solution without consideration of asperity merger. It is seen that the asperity interaction effect is more than just the delay of contact as shown in the statistical model, it also contributes to the loss of linearity between the contact force and the contact area. Our model also shows that: for elastic contact, using spherical asperities results in a larger average contact pressure than using sinusoids; when plasticity is taken into account, using a sphere to represent asperities results in a softer response as compared with using sinusoids. It is also confirmed that sinusoidal asperities are a much better description than spheres, by comparison with fully resolved FEM simulation results for computer-generated rough surfaces.
[DOI: 10.1115/1.4044635]

Keywords: discrete GW model, Hertz solution, asperity interaction, plasticity, contact area, surface roughness and asperities

1 Introduction

A rough surface, at a small length scale, is seen to consist of asperities whose geometrical properties (e.g., height, size, etc.) are stochastically distributed. These asperities play a key role in surface engineering problems related to contact, such as conductance of electrical component [1], or friction and wear [2,3]. Therefore, it is vital to understand the mechanical responses of these asperities. However, the complexity of the rough surface contact problem lies in the fact that the overall surface behavior is the result of all asperities that are involved during the contact. Therefore, a reasonable prediction not only requires the accurate description of geometrical properties and mechanical behavior of individual asperities but also the interaction among asperities during the deformation.

By far, one of the best-known theories for modeling rough surface contact is the statistical Greenwood and Williamson (GW) method [4]. The theory treats asperities as half sphere of the same size, and the height of these asperities follows a Gaussian or exponential distribution. Furthermore, it is assumed that the overall deformation is small such that neighboring asperities do not interact elastically. Mechanical response of spherical asperities is described by the classic Hertz solution in contact mechanics [5], $F_s = \frac{4}{3}E^*R^{1/2}\delta^{3/2}$, where F_s is the contact force of a single asperity, E^* is the equivalent Young's modulus, R is the radius of the sphere, and δ is the deformation. The GW model successfully predicts the linear dependence of the real contact area on the contact (normal) force. However, the assumptions of the GW model are very strong and for most situations quite unrealistic, which is why a number of researchers tried to relax these assumptions.

On one hand, regarding the asperity geometry, for example, Bush et al. [6] generalized spherical asperities to be paraboloids with the same principal curvatures and applied the classical Hertz solution for their deformation. The model is known as BGT model and predicts a linear relationship between the contact force and the contact area: $F/(E^*A_{nom}) = \sqrt{m_2/\pi}\cdot(A/A_{nom})$ where A_{nom} is the surface nominal area and m_2 is the surface spectrum moment. Rough surface profile measurements [7] clearly show that a sinusoidal description is much more realistic than a circular asperity geometry. Moreover, also from a computational point of view, a sinusoid is better than a half sphere: the sharp corner between the half sphere and the substrate creates stress concentrations which become problematic when considering plasticity. Sinusoids, on the other hand,

[1]Corresponding authors.

Contributed by the Tribology Division of ASME for publication in the Journal of Tribology. Manuscript received February 23, 2019; final manuscript received August 7, 2019; published online September 5, 2019. Assoc. Editor: Bart Raeymaekers.

do not have such problems because of the C1 continuity at the asperity base. Indeed, the sinusoidal description of the asperity geometry has been used in many studies of the mechanical response of single asperities [8–10]. Through finite element method (FEM) simulations, Saha et al. [11] recently analyzed the flattening of a three-dimensional sinusoidal asperity and provided an empirical expression for the average pressure that causes complete contact. For the elastic contact, almost all studies that considered sinusoidal asperities took the Hertz solution as the reference solution based on the argument that the asperity tip can be treated as a spherical tip. Unfortunately, it is not clear when the deformed asperity shape would violate the assumption of a spherical shape. This emphasizes the necessity of a Hertz-like analytical solution for the mechanical response of a single sinusoidal asperity.

On the other hand, with respect to the asperity interaction, for instance, Ciavarella et al. [12] included asperity interactions through treating the contact pressures as uniformly distributed over the apparent contact area and calculating the resulting deformation. Their correction is equivalent to an increase of the effective separation between the rigid flat and asperity mean height by a quantity proportional to the nominal pressure. Song et al. [13] used a statistical approach to find neighboring asperities of the asperity under contact and to effectively adjust the mean plane separation. All the above attempts, regardless of their assumptions and accuracy of their results, highlighted the importance of asperities interactions. All above models have problems in common: (i) the interaction effect is averaged across the surface which is the only option for a statistical model and (ii) the effect of asperity interaction in a statistical model is mainly reflected as the delay of contact. However, the interaction effect is physically highly localized and the effect decays with the increasing distance to the contacting asperity. The asperity interaction effect is more than just the delay of the contact: the interaction would change the asperity height distribution, therefore the distribution of local contact points/regions. In order to capture the localized feature of the asperity interaction and the change of asperity height distribution, a discrete model is necessary.

Regarding the plastic deformation of an asperity, Kogut and Etsion [14] proposed fitting formulas for contact force and contact area based on a FEM simulation of a half sphere whose base is fixed. Then, the fitting formulas are used in the statistical GW model to predict the surface contact response. Following the same idea, Song et al. [15] studied the effect of size-dependent plasticity on the rough surface contact behaviors. However, the FEM-based single asperity response strongly depends on the model geometry and boundary conditions. It is clear that using a sphere to represent realistic surface asperities becomes inappropriate when the deformation exceeds a certain range, i.e., the argument of equivalent curvature radius fails. Moreover, different shapes of asperities could have the same equivalent curvature radius; however, they may have a different mechanical response when considering plasticity. Furthermore, the commonly used boundary condition in FEM simulations of a half sphere is also debatable: fixing the bottom of the half sphere will artificially stiffen the asperity response while asperities are assumed to stand on a half infinite domain in the GW statistical modeling.

In this paper, we propose a discrete GW model of rough surface contact that includes three main improvements as compared with the existing GW-type models. First, the asperity shape is chosen to be sinusoidal, which is more realistic than the spherical shape. An analytical solution of sinusoidal asperity contact is derived. Second, the asperity interaction effect is obtained in a discrete GW model during the contact utilizing a modified Boussinesq solution. Third, plasticity is considered based on FEM simulations of a single asperity sitting on a large enough substrate. The effect of plasticity and choice of asperity shape in the discrete GW model are discussed based on the comparison with fully resolved FEM simulations of computer-generated rough surfaces. The remainder of this paper is organized as follows: Sec. 2 describes the analytical solution for sinusoidal asperity under contact and comparison with FEM solution. Section 3 is focused on the effect of the asperity shape (sinusoidal versus spherical) on the rough surface elastic contact behavior. Section 4 is focused on the elastic interaction and the influence of the asperity interaction effect on the rough surface response under contact. In Sec. 5, we focus on the effect of plasticity on the asperity response and discuss the problems of using spheres. Moreover, discrete GW model results are compared with full-detail FEM simulation results. In Sec. 6, we summarize our results. In Appendices A and C, we describe in detail the derivation of the analytical solution of the sinusoidal asperity under contact. We discuss the difference between asperity indentation and asperity flattening problems which are the two options for simplifications of two rough surface contact problems in Appendix B. Details of fitting parameters of asperity elastic–plastic response are shown in Appendix D.

2 Elastic Response of a Three-Dimensional Sinusoidal Asperity Under Contact

2.1 Analytical Solution for a Sinusoidal Asperity Under Contact. In what follows, an analytical solution is obtained for the elastic response of a three-dimensional sinusoidal asperity flattened by a rigid platen which is carried out as shown in Fig. 1 (2D profile). The surface profile of the sinusoidal asperity is given by

$$z(x)=\frac{1}{2}h\left[\cos\left(\frac{2\pi}{\lambda}x\right)+1\right] \tag{1}$$

where h and λ represent the height and width of the asperity, respectively. The radius of curvature at the tip of the sinusoidal asperity is $R=\lambda^2/(2\pi^2 h)$.

According to Johnson [5], for the axisymmetric case, the distance between rigid flat and the asperity surface $g(x)$ can be approximated through a Taylor expansion in the form of $\Sigma A_n x^{2n}$ where n is the order of the expansion and A_n is the expansion coefficient (for more details, see Appendix A). For $n=1$, the solution has the form:

$$F_s=\frac{2\sqrt{2}}{3}\frac{\lambda}{\pi\sqrt{h}}E^*\delta^{3/2},\quad A_s=\frac{\lambda^2}{2\pi h}\delta \tag{2}$$

where F_s is the contact force of the asperity and A_s is the contact area. The solution is essentially the classical Hertz solution if one substitutes $R=\lambda^2/(2\pi^2 h)$ into Hertz solution $F_s=\frac{4}{3}E^*R^{1/2}\delta^{3/2}$. When the value of n is 2, the analytical results (from now on, we term it "extended Hertz solution") become

$$F_s=2\sqrt{6}E^*\frac{h\lambda}{\pi}\left(\frac{3}{4}-\sqrt{\frac{9}{16}-\frac{1}{2}\frac{\delta}{h}}\right)^{3/2}-\frac{8}{5}\sqrt{6}E^*\frac{h\lambda}{\pi}\left(\frac{3}{4}-\sqrt{\frac{9}{16}-\frac{1}{2}\frac{\delta}{h}}\right)^{5/2}$$

$$A_s=\frac{3\lambda^2}{2\pi}\left(\frac{3}{4}-\sqrt{\frac{9}{16}-\frac{1}{2}\frac{\delta}{h}}\right) \tag{3}$$

Even higher orders of the expansion have been checked numerically. The results show that the deviation between the extended Hertz solution ($n=2$) and higher-order expansions ($n\geq 3$) is not

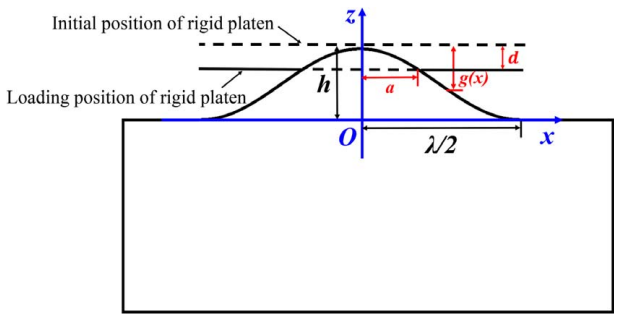

Fig. 1 Schematic of the problem: an elastic sinusoidal asperity on the substrate is flattened by a rigid platen

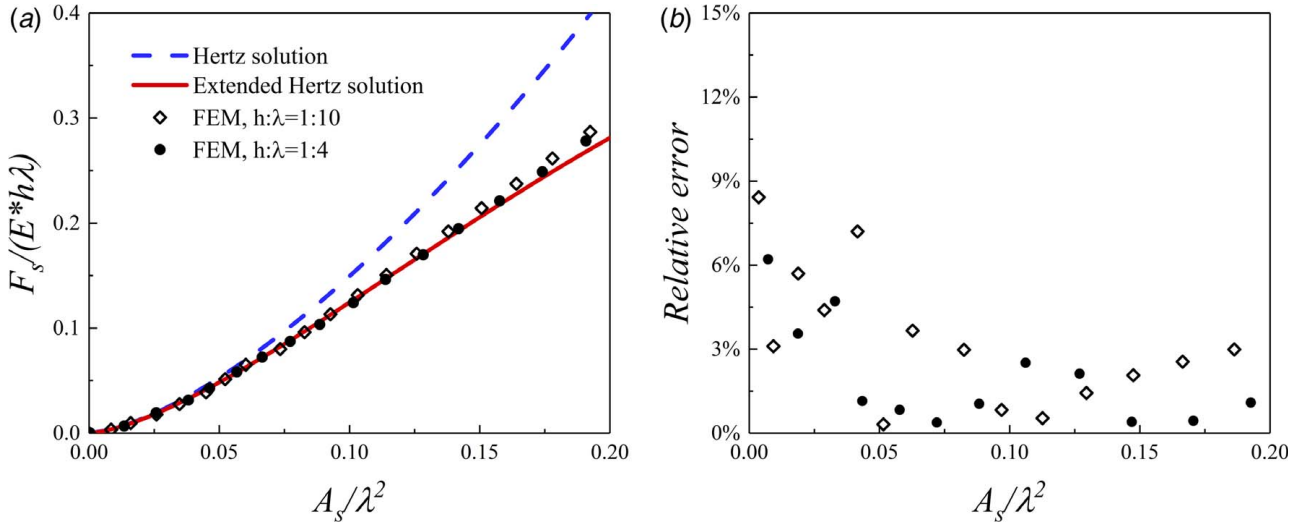

Fig. 2 (*a*) Comparison of Hertz and extended hertz solution with FEM results and (*b*) relative error of extended Hertz solutions compared with FEM results (marker symbols as in (*a*))

significant within the loading range under consideration, therefore we will use $n = 2$.

2.2 Verification of the Extended Hertz Solution Through Finite Element Method. To validate the analytical results, an axisymmetric asperity with a sinusoidal profile is located on the substrate and is compressed by a rigid platen. The solid mechanical boundary value problem is solved by the commercial finite element package ABAQUS [16]. The material of the asperity and the substrate are the same and are idealized as purely elastic, with the Young's modulus taken as 1, and the Poisson's ratio taken as 0.3. Boundary effects are eliminated by using large dimensions for the substrate and the substrate can be regarded as a half infinite domain. In our simulation, the size of the substrate is taken to be $\max\{20h, 20\lambda\}$ (more details are in Appendix B). Simulations with different asperity height-to-wavelength ratios ($h/\lambda = 0.1$, 0.25) were carried out. The contact force F_s and the contact area A_s of the asperity are normalized through $F^* = F_s/(E^*h\lambda)$ and $A^* = A_s/\lambda^2$ to eliminate the asperity geometry effect. The results in Fig. 2 show that at small load levels, both the Hertz solution ($n = 1$) and the extended Hertz solution ($n = 2$) agree well with the FEM results. However, with increasing deformation, the Hertz solution increasingly deviates from the FEM results. The reason is that the estimate of the radius of curvature at the asperity tip is not adequate anymore. This indicates that using Hertz solution describing sinusoidal asperity response is only valid for small load. By contrast, the extended Hertz solution still matches the FEM results very well and only slightly deviates in the high loading regime.

The reason for these deviations is that for high load levels, the deformation of the substrate starts to influence the resulting deformation of the asperity. As shown in Fig. 1, the total displacement d is accommodated by the deformation of the asperity δ and the deformation of the substrate u_z (Eq. (4)), where only the former is considered in the analytical solution

$$d = \delta + u_z \tag{4}$$

Therefore, we utilize the deviation to quantify the substrate deformation under the asperity as the function of the contact force in the form of

$$u_z = C \cdot \frac{1-\nu^2}{\pi E a} \cdot F_s \tag{5}$$

where C is the fitting parameter and a is the contact radius which can be calculated through the contact area A_s. The linear fitting parameter C for different shapes of asperities is shown in Fig. 3,

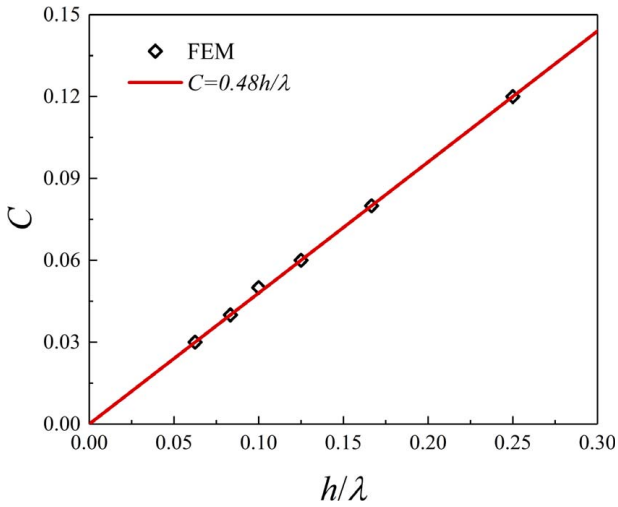

Fig. 3 Fitting parameter C versus wavelength-to-amplitude ratio. In our FEM simulations, the ratio of amplitude–to-wavelength has been restricted to $0.01 < h/\lambda < 0.3$, which covers most of the asperity shapes in realistic engineering surfaces [10]

where $C = 0.48 \cdot h/\lambda$. Subsequently, the extended Hertz solution considering the deformation of the asperity base as described in Eq. (5) will be used to describe the single asperity response as follows (more details can be found in Appendix C):

$$A_s = \pi \cdot \frac{\left(\frac{2h}{25\lambda}+\frac{1}{4}\right) - \sqrt{\left(\frac{2h}{25\lambda}+\frac{1}{4}\right)^2 - \frac{2}{3}\left(\frac{4h}{125\lambda}+\frac{1}{12}\right)\frac{d}{h}}}{\frac{8}{3}\frac{\pi^2}{\lambda^2}\left(\frac{4h}{125\lambda}+\frac{1}{12}\right)} \tag{6}$$

$$F_s = \frac{8}{3} \cdot E^* \frac{h\pi^{1/2}}{\lambda^2} A_s^{3/2} - \frac{64}{45} \cdot E^* \frac{h\pi^{3/2}}{\lambda^4} A_s^{5/2}$$

3 Discrete Modeling of a Rough Surface With Sinusoidal Asperities

In Sec. 2, we addressed the consequence of using Hertz solution to describe single sinusoidal asperity mechanical response. In this section, we focus on the consequences of using the Hertz solution

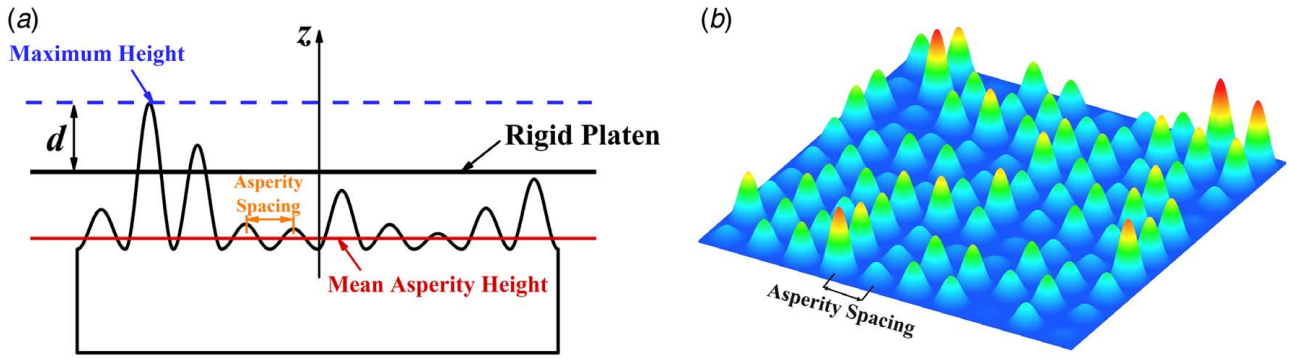

Fig. 4 (*a*) Schematic of the problem: asperities are flattened by a rigid platen and (*b*) example of a rough surface

for sinusoidal asperities on a rough surface under contact loading. The contact of the surface is analyzed through discrete GW modeling: the surface consists of N asperities that are placed on a regular grid—an approach typical for statistical models also used for studying friction phenomena [17–19]—and whose height follows a Gaussian distribution with the average value $\bar{h}$ and standard deviation σ. As shown in Fig. 4(*a*), the rigid platen is initially positioned at the highest asperity peak, and the loading distance is d. The contact force and area can be calculated by $F = \sum_{i=1}^{N} F_i$, $A = \sum_{i=1}^{N} A_i$, where F_i and A_i are the contact force and the contact area of each single asperity i, and they can be calculated following Sec. 2.1 depending on the asperity shape. For the rough surface shown in Fig. 4(*b*), we assume that all asperities have the same base width λ, but different height. We define the surface roughness parameter as $\beta = \sigma/\bar{h}$, i.e., the ratio between standard deviation and average of the Gaussian distribution.

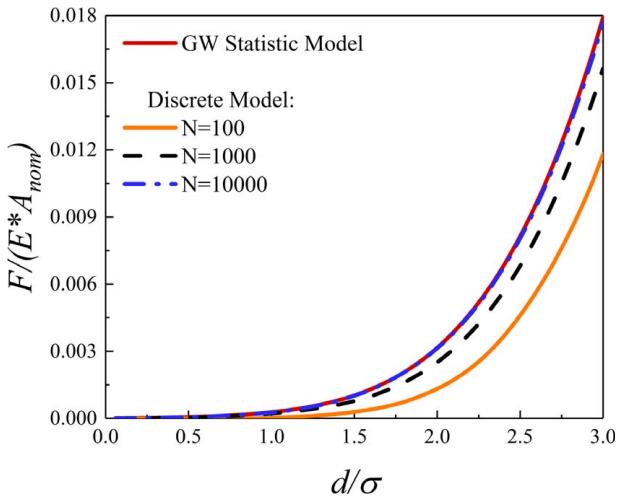

Fig. 5 Effect of the number of asperities in the discrete GW model

The influence of randomness decreases as the number of asperities increases, ultimately recovering a Gaussian distribution in terms of heights. As can be seen in Fig. 5, when the number of asperities is chosen as $N = 10{,}000$ in the discrete GW model, the agreement with the statistical GW model is nearly perfect. Therefore, $N = 10,000$ is used in the discrete model hereafter.

For a rough surface ($\beta = 0.5$ and $\bar{h}{:}\lambda = 1{:}6$), it can be seen in Fig. 6(*a*) that using the Hertz solution for sinusoidal asperities yields a slightly smaller contact force for the same loading magnitude, at the same time a slightly smaller contact area (shown in the inset). However, the contact pressure which is the ratio of the contact force to the contact area is larger than using the extended Hertz solution.

Derived from the assumption of the full contact at all length scales, Persson's contact model [20] can also provide good predictions for

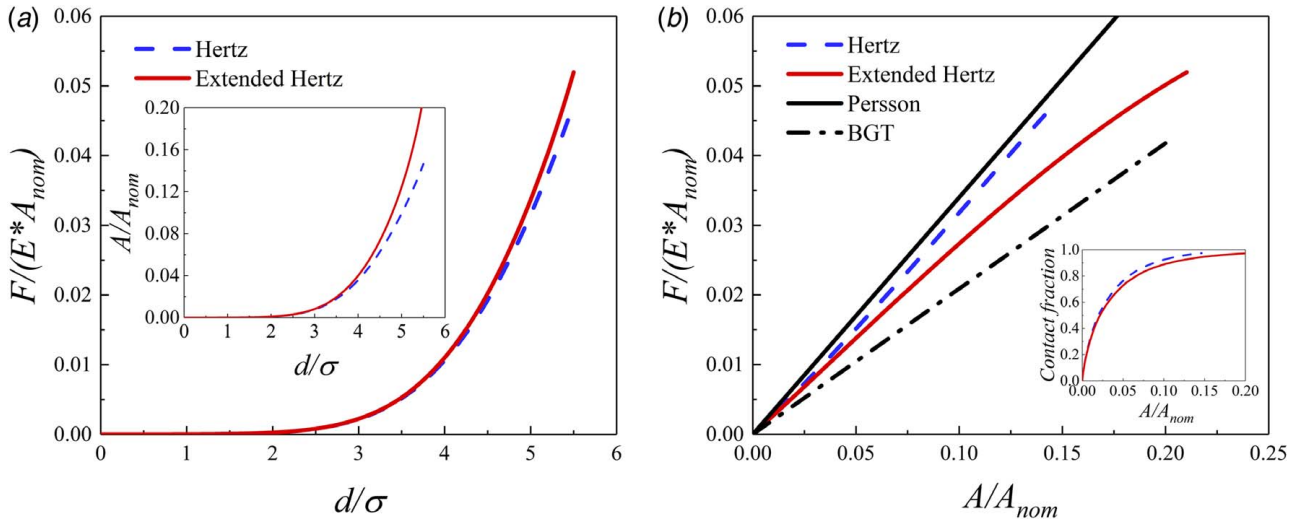

Fig. 6 Comparison of the discrete GW model results using different asperity shapes. (*a*) Force versus displacement. The inset shows the evolution of the contact area with increasing loading displacement. (*b*) The ratio between normalized contact force and normalized contact area. The inset shows the evolution of contact fraction (i.e., the number of asperities in contact normalized by the total number of asperities) for increasing contact area

rough surface contact problem, especially close to full contact. The model [20,21] predicts a linear relationship between the contact force and the contact area: $F/(E^*A_{nom}) = \sqrt{\pi m_2/4} \cdot (A/A_{nom})$, while the BGT model [6,21] predicts another linear dependence $F/(E^*A_{nom}) = \sqrt{m_2/\pi} \cdot (A/A_{nom})$. For surfaces with isotropic roughness morphology, m_2 can be calculated as $AVG[(dz(x)/dx)^2]$ [22], where $z(x)$ indicates a cross section along an arbitrary x direction of the 3D surface and AVG stands for the arithmetic average. For the surface roughness parameter chosen above, both results using Hertz and using extended Hertz lie in between the predictions of the Persson and BGT models, and the Hertz solution predicts a higher contact pressure than the extended Hertz solution which will result in more differences when plasticity is considered as well. It is also worthy to notice that, in the inset of Fig. 6(*b*), for the same total contact area, using the Hertz solution will result in slightly more asperities in contact. This again emphasizes the importance of accuracy of the single asperity mechanical response which influences the contact morphology of the whole surface.

4 Asperity Interaction

4.1 Asperity Interaction Model. One of the fundamental assumptions of the GW model is that the deformation of a single asperity happens independently from the deformation of other asperities. In this section, we include asperity interaction by considering elastic deformation of a single asperity base caused by all other asperities under contact. The advantage of the discrete GW model is that it is possible to precisely determine the elastic interaction rather than the average shift of the asperity height as done in the statistical manner. Instead of using the displacement solution for the substrate deformation from the Hertz theory, we use the Boussinesq solution [5] for the displacement field caused by a concentrated force. The choice of using a point force solution instead of the Hertz theory is based on the following reason: asperity interaction is essentially the elastic interaction of the surface substrate (where all asperities are located). The Hertz theory requires the distribution of the contact pressure to determine the displacement field, even though the contact pressure distribution is known at the contact (asperity tip); however, it is not known at the substrate (asperity base). Assumptions in some studies [13,23,24] about the pressure distribution at the substrate even violates the force equilibrium. The Boussinesq solution has the form $u_i^{int} = ((1-\nu^2)/\pi E r_{ij})F_j$, where u_i is the substrate displacement under asperity i caused by an asperity j under contact whose contact force is F_j, and r_{ij} is the distance between the two asperities. The accuracy of using the Boussinesq solution for the asperity interaction effect has been

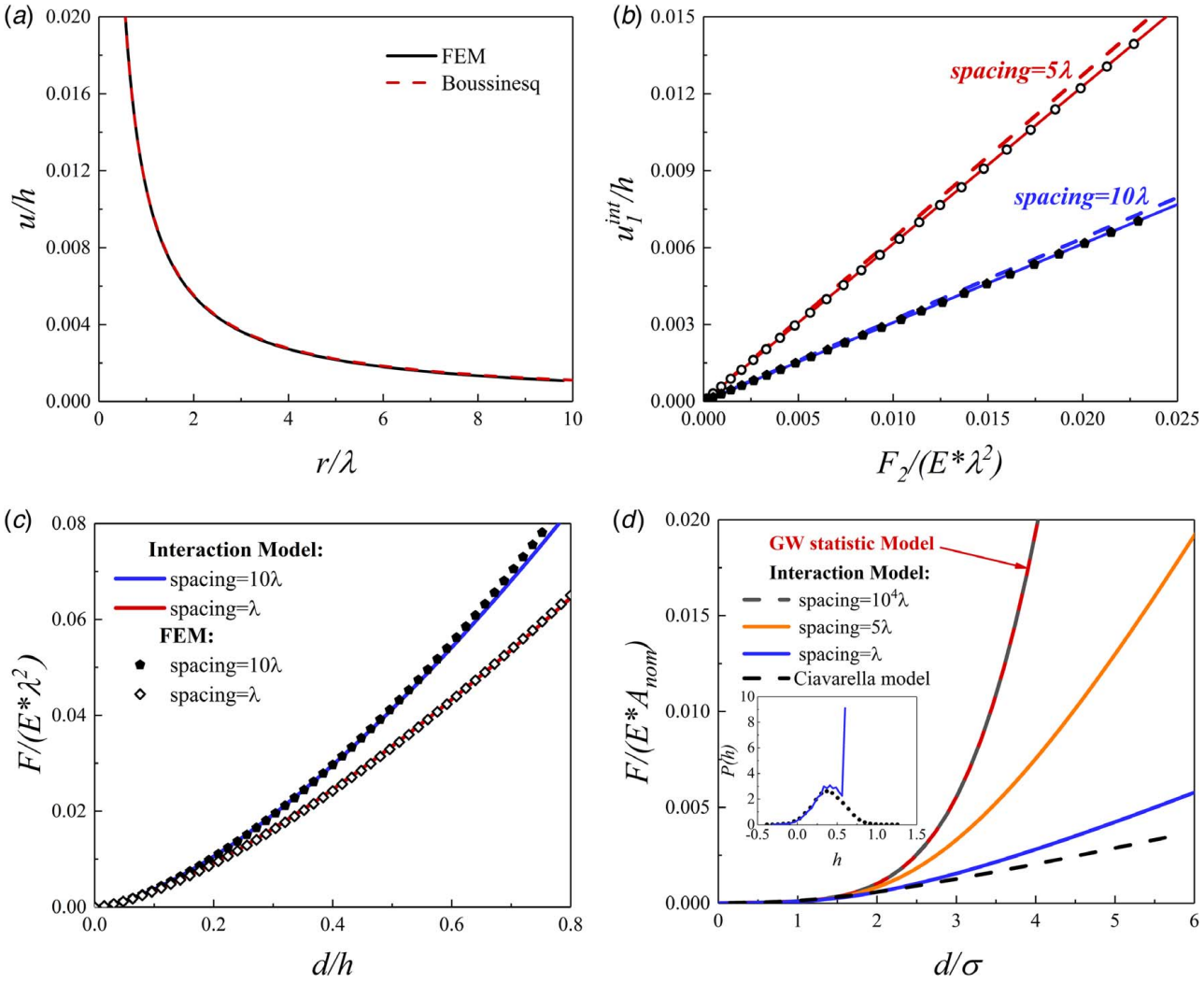

Fig. 7 (*a*) Comparison of the displacement from FEM and Boussinesq solution, where *r* is measured from the center of the asperity base; (*b*) for two asperities, displacement on the tip of one asperity due to the interaction of the other asperity under contact; (*c*) verification of the proposed interaction model: comparison with FEM results ($N = 4$) for two different asperity spacing; and (*d*) the effect of asperity spacing and comparison with Ciavarella's model. The inset shows the asperity height distribution when the load is $d/\sigma = 5$. Solid line of the inset 5/λ; dots lines of the inset–Ciavarella model.

verified in an experiment where a rigid patterned indenter indents a softer flat surface [25]. Here, for the asperity flattening problem shown in Fig. 7(*a*), where the displacement filed around an asperity under contact is plotted against the Boussinesq solution, we can see that Boussinesq solution matches the FEM solution very well. Moreover, in Fig. 7(*b*), for two sinusoidal asperities (numbered as 1 and 2) of certain spacing on a large substrate, asperity 2 is flattening and the displacement at the tip of asperity 1 is recorded. When the contact force is large, the Boussinesq solution and the FEM result start to deviate. The reason is that when the contact force at the asperity tip is large, the stress distribution at the asperity base starts to violate the assumption of a concentrated force acting at the asperity base. Since the deviations are approximately linear, we propose a correcting factor k such that the displacements become

$$u_i^{int} = k \cdot \frac{1-\nu^2}{\pi E r_{ij}} \cdot F_j \tag{7}$$

According to simulations with different asperity height wavelength ratios and different asperity, spacing k is taken as 0.9656, which is still close to one. This means that the Boussinesq solution works well for the asperity shape and spacing under consideration in this paper. Clearly, when the asperity spacing is so small that asperity merge/coalesce has to be taken into account, the Boussinesq solution would fail to capture the interaction effect.

Any displacement at the asperity tip u_i consists of two parts: the displacement u_i^{self} caused by the contact force F_i and the displacement u_i^{int} caused by contact forces $F_j (j = 1, 2, \ldots N, j \neq i)$ of other asperities. In each loading increment, we determine the resulting contact forces and asperity displacements iteratively through the conjugate gradient method where the residual value r_i of each asperity is defined as $r_i = d_i - u_i^{int} - u_i^{self}$, and d_i is the loading displacement. In order to check the accuracy of the above proposed method, a comparison with FEM simulation of four asperities is carried out. In the FEM simulation, four sinusoids on a large substrate are flattened, the results are shown in Fig. 7(*c*) for two different asperity spacing. It is seen that the our asperity interaction model is in good agreement with the FEM simulations.

For surfaces with the same number of asperities ($N = 10{,}000$ in the discrete GW model) and roughness, the effect of the asperity spacing is shown in Fig. 7(*d*): when the asperities are very far away from each other, interaction effects disappears; the effect of asperity interaction increases with decreasing asperity spacing. For close-packaged asperities (the spacing between two asperity tip is λ), the interaction effect is expected to be the strongest. However, the interaction model proposed by Ciavarella et al. [12] predicts an even stronger effect of asperity interaction. The reason is that in Ciavarella's model, the asperity interaction is considered as the equivalent shifting of the whole surface. As an effect, the asperity height distribution still is a Gaussian distribution and

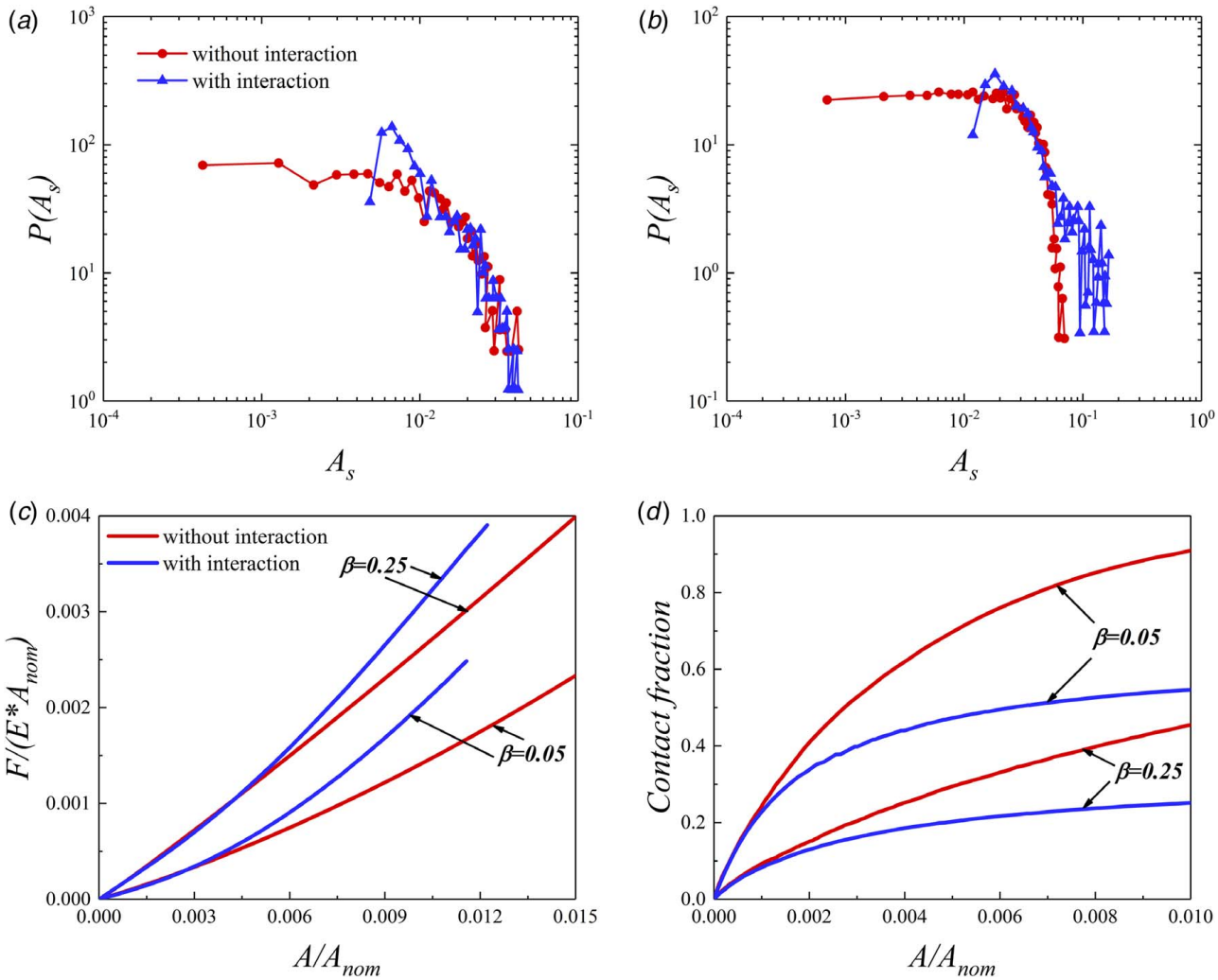

Fig. 8 Probability density distribution of single asperity contact areas for model ($\beta = 0.25$) with and without asperity interaction effect. (*a*) Small nominal contact ($A/A_{nom} = 0.1\%$); (*b*) large nominal contact area ($A/A_{nom} = 1\%$); (*c*) dependence of the normalized contact force on the normalized contact area for two different rough surfaces, with and without asperity interaction; and (*d*) evolution of the contact fraction, i.e., how many asperities from all asperities on the surface are in contact

only the average shifts. By contrast, our asperity interaction model implemented through discrete GW model clearly shows that this is not the case (shown in the inset when $d/\sigma = 5$), the asperity height distribution deviates from the Gaussian distribution, and there are fewer high asperities than they are in Ciavarella's model. Hence, Ciavarella's model overestimated the effect of asperity interactions.

Besides the effect on the contact force, the asperity interaction has another important effect on the contact area distribution which cannot be studied in a statistical model. For the same total contact area, we analyze how the contact area is distributed in the model with interaction and without interaction. Figures 8(*a*) and 8(*b*) show the probability density distribution of the single asperity contact area for different total contact area. It can be seen that, when the total contact area is small, no clear difference is found as the interaction effect is still quite limited (the difference is only the smaller size distribution which does not dominate the overall contact behavior). However, when the total contact area is larger, the probability density distribution is very different: in the model with interaction effects, there are many more larger contact areas, i.e., loading is mainly accommodated by few asperities. The distribution clearly reflects the physical process during the contact: when considering interaction effect, contacting asperities tend to delay/avoid forming new contacts, the increase of the contact load and area is accommodated by increasing the contact area of existing contact points. This is also consistent with the result in Fig. 8(*c*) and shows in the linearity: in the GW-type model, the linearity requires the increase of the number of contacts during the loading. This affects the surface height statistics, since interaction effects forces the existing contact to accommodate the increasing load. This delays the increase of contact area, which is responsible for the loss of linearity. In Fig. 8(*d*) which shows the contact fraction, we can see that the contact fraction tends to converge to a smaller value in the model with interaction, i.e., the asperity interaction effect acts as to avoid forming new contacts which will lead to a larger contact fraction. Moreover, it is seen that rougher surfaces (larger β) result in a larger contact pressure (the slope of the plotted curves in Fig. 8(*c*)) and less contacts (Fig. 8(*d*)) which means that it is more difficult to completely seal an elastic rougher surface.

5 The Effect of Plasticity on Single Asperity Response and the Rough Surface Contact Behavior

In the previous sections, we have discussed the effect of the asperity shape. In this section, we revisit the effect of the asperity shape when plasticity is considered. For sinusoidal asperities, the model geometry and boundary condition is the same as in Figs. 1 and 12. As a material model, we use a J2 plasticity model with the yield strength $Y = 200$ MPa. The Young's modulus is chosen

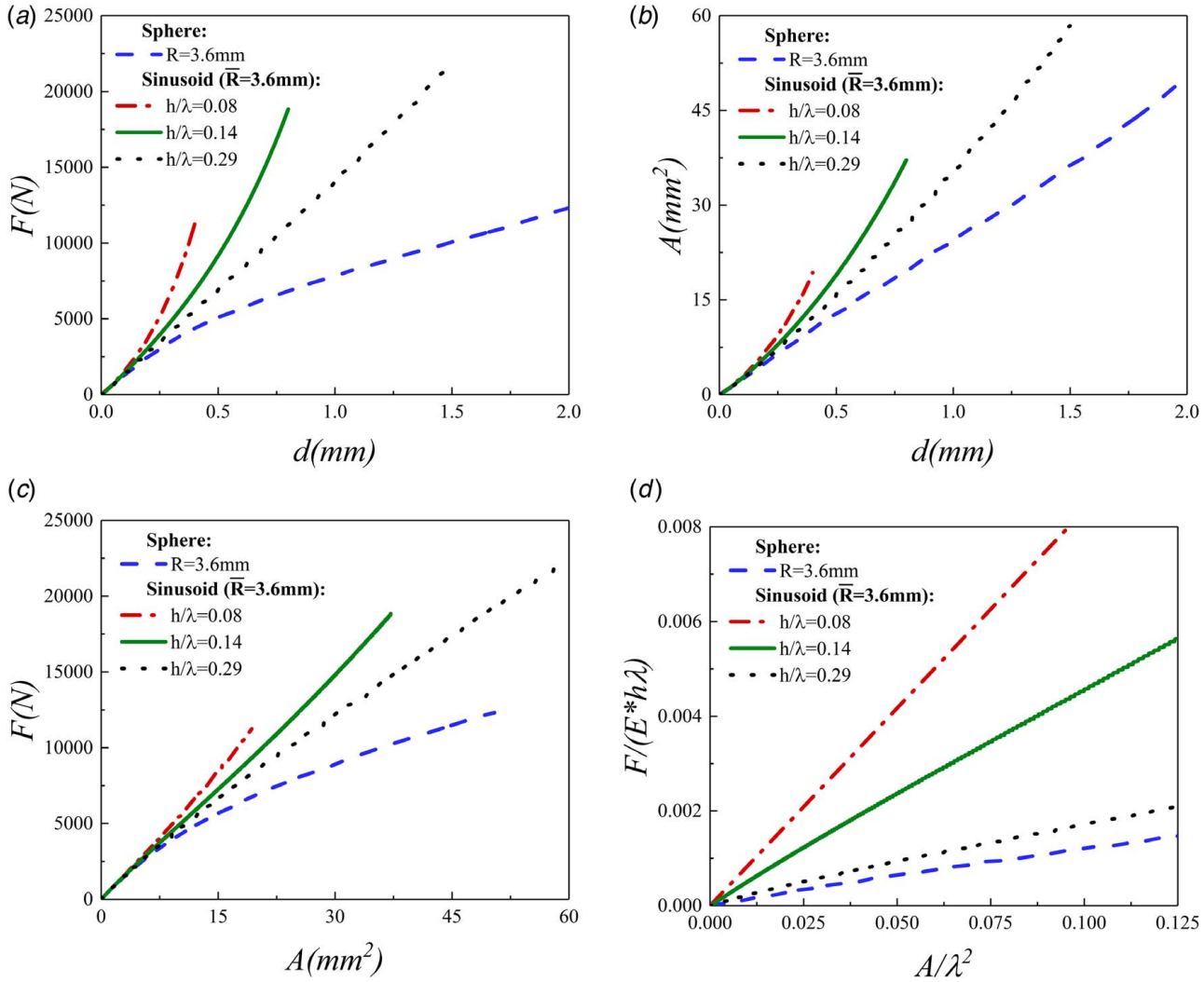

Fig. 9 Effect of the asperity shape on the asperity response considering plasticity. (*a*) Contact force as the function of the loading distance; (*b*) contact area as the function of the loading distance; (c) contact force as the function of the contact area; and (*d*) normalized contact force versus normalized contact area

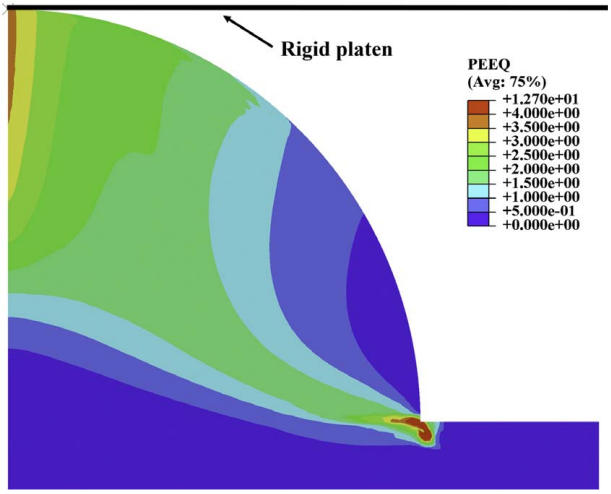

Fig. 10 Stress concentration of spherical model causes plasticity at the corner, only a small portion of the substrate is shown here

to be 70 GPa, and the Poisson's ratio is 0.33. Several shapes and sizes of sinusoidal asperities are studied: $\lambda = 6$ mm, 10 mm, 20.9 mm along with $h/\lambda = 0.08$, 0.14, 0.29. The common feature of these sinusoids is that they have the same radius of curvature, $R = 3.6$ mm, at the asperity tip. It can be seen in Fig. 9 that the mechanical response of an asperity is very sensitive to its shape. Unlike the results in Fig. 2(*a*), the normalized asperity response shown in Fig. 9(*d*) for sinusoidal asperities still show strong dependence on the asperity geometry. This clearly indicates that replacing a sinusoidal asperity by a sphere that has the same radius of curvature becomes inappropriate when plasticity is taken into account.

Using a sphere instead of sinusoids also becomes problematic from the numerical point of view, as demonstrated by the equivalent plastic strain distribution in Fig. 10. There, the unphysical sharp corner between the spherical asperity base and the substrate creates stress concentrations which result in plastic deformation. Although the stress concentration could be solved by making profile modifications (rounding corners), however, special attention needs to be paid to the radius of the rounding. Some FEM models like those in Kogut and Etsion [14] avoided such problems by only considering a half sphere and fixing its base. However, this is contradictory to the assumption used later on in the GW model: asperities sit on the infinite large substrate.

It has been seen that the single asperity response is quite sensitive to its shape when plasticity is considered. This also indicates that in a rough surface contact problem, modeling surface asperities through spheres can result in significant deviations/errors. For example, for a computer-generated rough surface as shown in Fig. 11(*a*), it is clear that the asperities look more like sinusoids rather than spheres. The statistical information of asperities and full-detail FEM results of this surface under contact can be found in Song et al. [15]. In order to carry out a discrete GW modeling, we have chosen sinusoids of different shapes and spheres that have the corresponding radius of curvature for those sinusoids. The details of Kogut and Etsion [14] type fitting of single asperity mechanical response can be found in Appendix D.

With fitted single asperity mechanical response and the asperity interaction method proposed in Sec. 4, the mechanical responses of such surface is then modeled through our discrete GW model. The results are compared with full-detail FEM simulation results (see Ref. [15]) and shown in Fig. 11(*b*). It can be seen that for purely elastic contact, within the loading range considered here, no clear difference is observed between using spheres and using sinusoids, because the contact area is small. In contrast, when plasticity is considered, using spherical asperities results in large deviation from FEM simulation results. Thus, representing surface asperities as spheres should be avoided.

6 Conclusions

In this paper, we proposed a discrete GW contact model which utilizes single asperity mechanical response and takes the asperity interaction into account. The salient conclusions of the study are:

(1) An analytical solution is first derived for flattening of a purely elastic sinusoidal asperity. Furthermore, the substrate deformation, which cannot be neglected for high load, is also taken into account. The analytical solution is implemented into the discrete GW model for rough surface contact. The commonly used spherical contact model is not valid anymore at high load level, neither for the single asperity nor for the rough contact.
(2) The interaction between neighboring asperities is taken into account by using the Boussinesq solution. For elastic contact of rough surfaces, the previous interaction model proposed by Civarella et al. [12] overestimates the interaction effect and predicts a lower stiffness than the accurate model, especially at high load. For the same total contact area, interaction effects may reduce the number of contact patches, but increase the area of the bigger contact patches.
(3) The elasto-plastic response of a single sinusoidal asperity strongly depends on the overall shape of the asperity. Therefore, it is inappropriate to use a sphere that has the same radius of curvature to represent the surface asperities. The

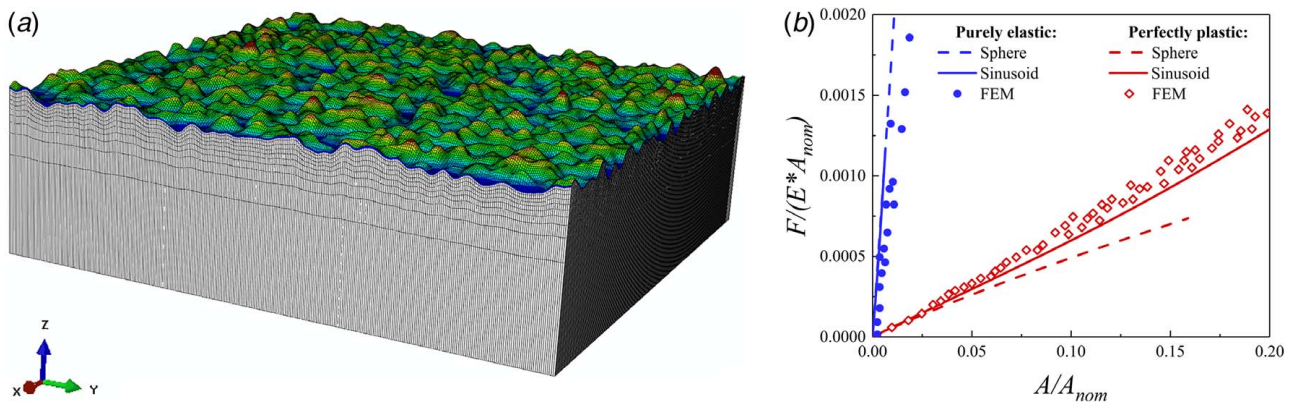

Fig. 11 (*a*) Numerically generated rough surface (more details in Ref. [15]). (*b*) Comparison of discrete GW modeling results with full-detail FEM simulation results for purely elastic and elastic–plastic contact.

consequence of using spheres to represent surface asperities is also clearly shown through the comparison between our discrete GW modeling results and full-detail FEM simulation results: spherical asperities significantly underestimate the contact pressure when the overall contact area is large.

To summarize, for elastic contact of the rough surface, our model is more accurate than statistical models [12,21] as the interaction effect is explicitly modeled. For elasto-plastic contact, the comparison between our model results and full-detail FEM simulation results, on the one hand clearly shows the accuracy of our model, on the other hand emphasizes the importance of a proper description of the asperity shape. Moreover, in terms of computational cost, our model performs much better than finite element based approaches: in a customized workstation (Intel Xeon 2.5 GHz 16 central processing units, 256 GB RAM), the full-detail FEM simulation of a rough surface as shown in Fig. 11(*a*) through ABAQUS took around 45 h, while the discrete GW model implemented by MATLAB took less than 5 min. It is therefore a very useful approach in particular in situations where systems of realistic dimensions and with a large number of asperities are to be considered.

Funding Data

- National Natural Science Foundation of China (Grant Nos. 11772334, 11572329, and 11672301; Funder ID: 10.13039/501100001809)
- National Key R&D Program of China (Grant No. 2017YFA0204402; Funder ID: 10.13039/501100012166)
- Youth Innovation Promotion Association CAS (Grant No. 2018022; Funder ID: 10.13039/501100004739)
- Strategic Priority Research Program of the Chinese Academy of Sciences (Grant No. XDB22040501)

Nomenclature

a = contact radius of a single asperity
d = loading displacement
h = height of a single sinusoidal asperity
k = correcting parameter
n = expansion order
r = distance from the point on the surface to the center of the asperity base
z = asperity height
A = contact area
C = fitting parameter
F = contact force
L = asperity base
N = total asperity number
R = radius of asperity summits
$\bar{h}$ = average height of asperities
b_1 = fitting parameter for elastic–plastic sinusoidal asperity
b_0 = fitting parameter for elastic–plastic spherical asperity with substrate
c_1 = fitting parameter for elastic–plastic sinusoidal asperity
c_0 = fitting parameter for elastic–plastic spherical asperity with substrate
m_1 = fitting parameter for elastic–plastic sinusoidal asperity
m_0 = fitting parameter for elastic–plastic spherical asperity with substrate
m_2 = spectral moment of the surface
n_1 = fitting parameter for elastic–plastic sinusoidal asperity
n_0 = fitting parameter for elastic–plastic spherical asperity with substrate
r_i = residual value
r_{ij} = the distance between asperity i and asperity j
u_i = the substrate displacement under asperity i
u_z = the substrate displacement of a single asperity
A_n = expansion coefficient
A_{nom} = nominal contact area
A_s = contact area of a single asperity
F_i = contact force of asperity i
F_j = contact force of asperity j
F_s = contact force of a single asperity
u_i^{int} = the displacement caused by the contact force F_j
u_i^{self} = the displacement caused by the contact force F_i
A^* = dimensionless contact area
E^* = equivalent Young's modulus
F^* = dimensionless contact force
β = surface roughness, $\sigma/\bar{h}$
δ = deformation of a single asperity
η = asperity areal density
λ = width of a single sinusoidal asperity
ν = Poisson's ratio
σ = standard deviation

Appendix A: Derivation of Analytical Solution of Elastic Contact

As shown in Fig. 1, the exact distance between the initial position of the rigid flat and the elastic sinusoidal profile is given by Eq. (A1) which can also be written in the form of Taylor expansion

$$g(x) = \frac{1}{2}h\left[1 - \cos\left(\frac{2\pi}{\lambda}x\right)\right] = A_1x^2 + A_2x^4 + A_3x^6 + \cdots \quad \text{(A1)}$$

where $A_1 = h(\pi/\lambda)^2$, $A_2 = -\frac{1}{3}h(\pi/\lambda)^4$, $A_3 = \frac{2}{45}h(\pi/\lambda)^6$ and so on, representing the expansion coefficient.

According to Johnson (Eqs. (5.20), (5.21), and (5.22) in Ref. [5]), in axisymmetric case, the contact force and the compression for a single asperity can be obtained through

$$F_s = \sum_{i=1}^{n} \frac{4A_nE^*na^{2n+1}}{(2n+1)} \frac{2\cdot 4\cdots 2n}{1\cdot 3\cdots(2n-1)}$$
$$\delta = \sum_{i=1}^{n} \frac{2\cdot 4\cdots 2n}{1\cdot 3\cdots(2n-1)} A_n a^{2n} \quad \text{(A2)}$$

where a is the contact radius, δ is the deformation of the asperity (which is the same as the displacement of rigid flat d if the deformation of the asperity base is ignored), and E^* represents the equivalent Young's modulus, defined as $(1/E^*) = ((1-\nu_1^2)/E_1) + ((1-\nu_2^2)/E_2)$, where E_1, E_2 and ν_1, ν_1 are Young's moduli and Poisson ratios of the two contacting materials, respectively. Thus, depending on the items used in the expansion, one can get contact area and contact force under the given load.

Appendix B: Comparison of Asperity Flattening and Asperity Indentation Models

For the problem of two rough surfaces contact, usually the problem is simplified into a flat surface contacts with a rough surface which has the equivalent roughness, and one of two surfaces is rigid, the other is deformable. If the flat surface is rigid, then the problem essentially becomes rough surface (asperity) flattening; if the rough surface is rigid, then the problem is indentation. Indeed, some GW-type models consider flattening problems, while others consider indentation problems. For example, Yin and Komvopoulos [25] simplified two rough surface contact problem into a rough indenter with a flat substrate while Kogut and Etsion [14] simplified the contact problem into the flattening of asperity. In our simulation, not only the flattening problem has been carried out, the indentation of a rigid sinusoidal asperity on a large flat elastic substrate has been carried out as well through FEM. Figure 12 shows an example of the employed mesh of the flattening and indentation models with the asperity dimension being $h = 1$ mm and $\lambda = 4$ mm and asperity base $L = 80$ mm.

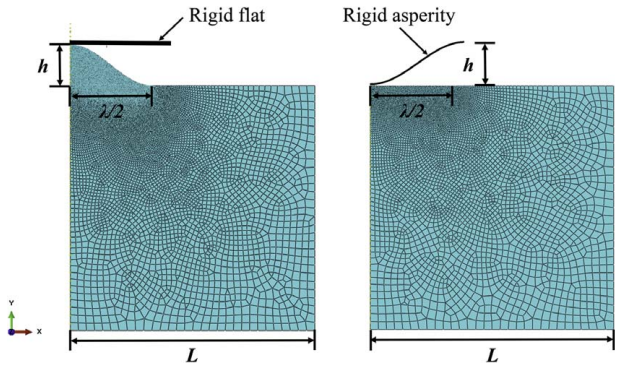

Fig. 12 Axisymmetric mesh example for left: flattening model and right: indentation model ($h = 1$ mm and $\lambda = 4$ mm)

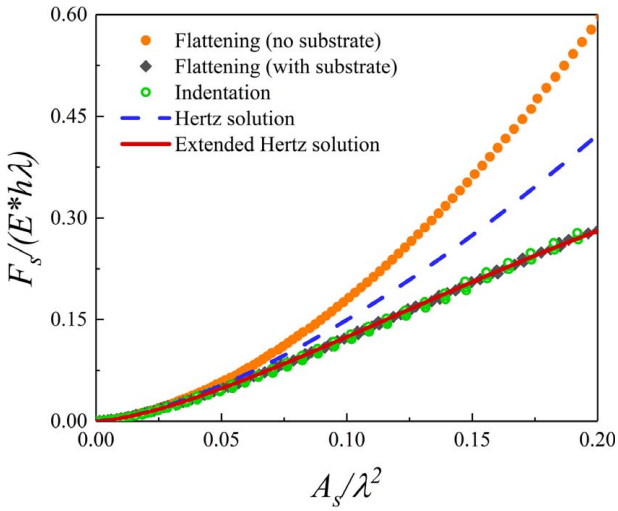

Fig. 13 Comparison between asperity flattening and indentation

It can be seen from Fig. 13 that the rigid sinusoidal asperity indentation problem is essentially the same with sinusoidal asperity flattened by a rigid flat which are the two choices of simplification for rough surface contact problems. However, one needs to be careful when choosing the flattening problem: the asperity needs to locate on a large enough substrate to utilize the Hertz-type solution which is based on half infinite assumption. When the contact force/area is large, the constraint at the asperity base strengthens the asperity (result shown in solid dots). This issue is ignored in most of the FEM studies of asperity flattening. Furthermore, it is also seen that using Hertz solution for a sinusoidal asperity is only valid at small loading.

Appendix C: Derivation of the Approximate Extended Hertz Solution Considering the Deformation of the Asperity Base

As stated in Sec. 2, when the load is large, the deformation of the substrate cannot be neglected. According to Eqs. (4) and (5), the deformation of a single asperity can be calculated by

$$\delta = d - 0.48 \cdot \frac{1-\nu^2}{\pi E a} \cdot F_s \tag{C1}$$

where d is the total loading displacement and F_s is the contact force of a single asperity.

The contact area can be obtained by substituting Eq. (C1) into extended Hertz solution (Eq. (3))

$$A_s = \frac{3\lambda^2}{2\pi}\left(\frac{3}{4} - \sqrt{\frac{9}{16} - \frac{d}{2h} + \frac{0.12}{E^*\lambda}\cdot\frac{F_s}{a}}\right) \tag{C2}$$

which can be written by

$$\frac{d}{2h} - \frac{\pi^2}{\lambda^2}a^2 + \frac{\pi^4}{9\lambda^2}a^4 = \frac{0.12}{E^*\lambda}\cdot\frac{F_s}{a} \tag{C3}$$

Substituting Eq. (C3) into extended Hertz solution (Eq. (3) in Sec. 2), a quadric equation can be derived

$$\frac{16\pi^4}{3\lambda^4}\left(\frac{4h}{125\lambda} + \frac{1}{12}\right)a^4 - \frac{4\pi^2}{\lambda^2}\left(\frac{2h}{25\lambda} + \frac{1}{4}\right)a^2 + \frac{d}{2h} = 0 \tag{C4}$$

As the relationship between a^2 and the total loading displacement d is monotonically increasing, negative roots should be neglected

$$a^2 = \frac{\left(\frac{2h}{25\lambda} + \frac{1}{4}\right) - \sqrt{\left(\frac{2h}{25\lambda} + \frac{1}{4}\right)^2 - \frac{2}{3}\left(\frac{4h}{125\lambda} + \frac{1}{12}\right)\frac{d}{h}}}{\frac{8}{3}\frac{\pi^2}{\lambda^2}\left(\frac{4h}{125\lambda} + \frac{1}{12}\right)} \tag{C5}$$

By using Eq. (C5), the extended Hertz solution considering the deformation of the asperity base can be obtained, which is Eq. (6) shown in Sec. 2.

Appendix D: Fittings of Asperity Mechanical Responses

Based on the numerically generated random rough surface (see Sec. 5) and its statistical parameters in Ref. [15], the surface morphology parameters of our discrete model are $rms = 0.08$ mm, and $\sigma = 0.039$ mm, which determine the value of average height ($\bar{h} = 0.07$ mm). The average asperity tip curvature $\bar{R}$ is 0.36 mm, so the fixed widths of each asperity can be calculated by: $\lambda = (2\pi^2\bar{h}\bar{R})^{1/2}$. According to the density of the rough surface ($\eta = 1.5\ \text{mm}^{-2}$), the nominal contact area can be determined by $A_{nom} = N/\eta$, where N is the number of asperities. As the height of asperities obeys Gaussian distribution, the height range of a single sinusoid is considered to be $\bar{h} \pm 3\sigma$. Based on the above parameters, the

Table 1 Fitting parameters of plastic sinusoidal asperities

	b_1	m_1	c_1	n_1
$0 \le \frac{d}{h} \le 0.2$	$0.003\left(\frac{h}{\lambda}\right)^{-1.055}$	$0.91\left(\frac{h}{\lambda}\right)^{-0.1}$	$0.44 + 0.86 \cdot \left(\frac{h}{\lambda}\right)$	$1.17\left(\frac{h}{\lambda}\right)^{0}$
$0.2 < \frac{d}{h} \le 0.4$	$0.005\left(\frac{h}{\lambda}\right)^{-0.912}$	$1.26\left(\frac{h}{\lambda}\right)^{0.001}$	$1.242\left(\frac{h}{\lambda}\right)^{0.286}$	$1.246 + 0.29 \cdot \left(\frac{h}{\lambda}\right)$
$0.4 < \frac{d}{h} \le 0.6$	$0.010\left(\frac{h}{\lambda}\right)^{-0.712}$	$2.207\left(\frac{h}{\lambda}\right)^{0.155}$	$1.903\left(\frac{h}{\lambda}\right)^{0.406}$	$1.295 + 1.3 \cdot \left(\frac{h}{\lambda}\right)$
$\frac{d}{h} > 0.6$	$0.017\left(\frac{h}{\lambda}\right)^{-0.546}$	$1.20 + 5.51 \cdot \left(\frac{h}{\lambda}\right)$	$0.45 + 3.41 \cdot \left(\frac{h}{\lambda}\right)$	$1.249 + 2.9 \cdot \left(\frac{h}{\lambda}\right)$

FEM-based elastic–plastic simulations for single asperity of different heights were carried out. Following the idea of Kogut and Etsion [14], for different shapes of sinusoids, we have fitted the asperity responses as the function of the loading distance in the form of

$$\frac{F_s}{E^* h\lambda} = b_1 \cdot \left(\frac{d}{h}\right)^{m_1}, \quad \frac{A_s}{\lambda^2} = c_1 \cdot \left(\frac{d}{h}\right)^{n_1} \tag{D1}$$

where the fitting parameters are functions of the asperity ratio. The entire elastic–plastic response is divided into four regimes, and the details of fitting parameters are shown in Table 1.

Similarly, using the corresponding radius curvature of the sinusoid tip and the same boundary conditions, the spherical asperity lying on a large substrate is also fitted, which has the form

$$\frac{F_s}{E^* R^2} = b_0 \cdot \left(\frac{d}{R}\right)^{m_0}, \quad \frac{A_s}{R^2} = c_0 \cdot \left(\frac{d}{R}\right)^{n_0} \tag{D2}$$

where the fitting parameters are $b_0 = 0.018$, $m_0 = 0.676$, $c_0 = 6.695$, and $n_0 = 0.98$.

References

[1] Zhai, C., Hanaor, D., Proust, G., Brassart, L., and Gan, Y., 2016, "Interfacial Electro-Mechanical Behaviour at Rough Surfaces," Extreme Mech. Lett., **9**(3), pp. 422–429.

[2] Zhai, C., Hanaor, D., and Gan, Y., 2017, "Contact Stiffness of Multiscale Surfaces by Truncation Analysis," Int. J. Mech. Sci., **131–132**, pp. 305–316.

[3] Gao, Z., Fu, W., Wang, W., Kang, W., and Liu, Y., 2018, "The Study of Anisotropic Rough Surfaces Contact Considering Lateral Contact and Interaction Between Asperities," Tribol. Int., **126**, pp. 270–282.

[4] Greenwood, J. A., and Williamson, J. B. P., 1966, "Contact of Nominally Flat Surfaces," Proc. R. Soc. A: Math. Phys. Eng. Sci., **295**(1442), pp. 300–319.

[5] Johnson, K. L., 1985, *Contact Mechanics*, Cambridge University Press, Cambridge.

[6] Bush, A. W., Gibson, R. D., and Thomas, T. R., 1975, "The Elastic Contact of Rough Surfaces," Wear, **35**(1), pp. 87–111.

[7] Poon, C. Y., and Bhushan, B., 1995, "Comparison of Surface Roughness Measurements by Stylus Profiler, AFM and Non-Contact Optical Profiler," Wear, **190**(1), pp. 76–88.

[8] Song, H., Dikken, R. J., Nicola, L., and Van der Giessen, E., 2015, "Plastic Ploughing of a Sinusoidal Asperity on a Rough Surface," ASME J. Appl. Mech, **82**(7), p. 071006.

[9] Sun, F., Van der Giessen, E., and Nicola, L., 2012, "Plastic Flattening of a Sinusoidal Metal Surface: A Discrete Dislocation Plasticity Study," Wear, **296**(1–2), pp. 672–680.

[10] Gao, Y. F., Bower, A. F., Kim, K. S., Lev, L., and Cheng, Y. T., 2006, "The Behavior of an Elastic–Perfectly Plastic Sinusoidal Surface Under Contact Loading," Wear, **261**(2), pp. 145–154.

[11] Saha, S., Xu, Y., and Jackson, R. L., 2016, "Perfectly Elastic Axisymmetric Sinusoidal Surface Asperity Contact," ASME. J. Tribol., **138**(3), p. 031401.

[12] Ciavarella, M., Greenwood, J. A., and Paggi, M., 2008, "Inclusion of "Interaction" in the Greenwood and Williamson Contact Theory," Wear, **265**(5–6), pp. 729–734.

[13] Song, H., Van der Giessen, E., and Vakis, A. I., 2016, "Erratum: Asperity Interaction and Substrate Deformation in Statistical Summation Models of Contact Between Rough Surfaces [Journal of Applied Mechanics, 2014, 81(4), p. 041012]," ASME J. Appl. Mech., **83**(8), p. 087001.

[14] Kogut, L., and Etsion, I., 2002, "Elastic-Plastic Contact Analysis of a Sphere and a Rigid Flat," ASME J. Appl. Mech., **69**(5), pp. 657–662.

[15] Song, H., Vakis, A. I., Liu, X., and Van der Giessen, E., 2017, "Statistical Model of Rough Surface Contact Accounting for Size-Dependent Plasticity and Asperity Interaction," J. Mech. Phys. Solids, **106**, pp. 1–14.

[16] Smith, 2014, *ABAQUS User's Maunual, Version 6.14*, Dassault Systemes Simula Corporation, Providence, RI.

[17] Afferrante, L., Bottiglione, F., Putignano, C., Persson, B. N. J., and Carbone, G., 2018, "Elastic Contact Mechanics of Randomly Rough Surfaces: An Assessment of Advanced Asperity Models and Persson's Theory," Tribol. Lett., **66**(2), p. 2.

[18] Persson, B. N. J., 2006, "Contact Mechanics for Randomly Rough Surfaces," Surf. Sci. Rep., **61**(4), pp. 201–227.

[19] Taloni, A., Benassi, A., Sandfeld, S., and Zapperi, S., 2015, "Scalar Model for Frictional Precursors Dynamics," Sci. Rep., **5**(8086), pp. 1–11.

[20] Persson, B. N. J., Bucher, F., and Chiaia, B., 2002, "Elastic Contact Between Randomly Rough Surfaces: Comparison of Theory With Numerical Results," Phys. Rev. B, **65**(18), p. 184106.

[21] Carbone, G., and Bottiglione, F., 2008, "Asperity Contact Theories: Do They Predict Linearity Between Contact Area and Load?," J. Mech. Phys. Solids, **56**(8), pp. 2555–2572.

[22] Kalin, M., Pogačnik, A., Etsion, I., and Raeymaekers, B., 2016, "Comparing Surface Topography Parameters of Rough Surfaces Obtained With Spectral Moments and Deterministic Methods," Tribol. Int., **93**, pp. 137–141.

[23] Chandrasekar, S., Eriten, M., and Polycarpou, A. A., 2012, "An Improved Model of Asperity Interaction in Normal Contact of Rough Surfaces," ASME J. Appl. Mech., **80**(1), p. 011025.

[24] Li, S., Yao, Q., Li, Q., Feng, X.-Q., and Gao, H., 2018, "Contact Stiffness of Regularly Patterned Multi-Asperity Interfaces," J. Mech. Phys. Solids, **111**, pp. 277–289.

[25] Yin, X., and Komvopoulos, K., 2012, "A Discrete Dislocation Plasticity Analysis of a Single-Crystal Semi-Infinite Medium Indented by a Rigid Surface Exhibiting Multi-Scale Roughness," Phil. Mag., **92**(24), pp. 2984–3005.